Paper No.
567

CORROSION 99

EFFECT OF CHLORIDE CONCENTRATION ON THE PITTING AND REPASSIVATION POTENTIALS OF REINFORCING STEEL IN ALKALINE SOLUTIONS

Lianfang Li , A. A. Sagüés
Dept. of Civil and Environmental Eng., College of Engineering
University of South Florida
4202 E. Fowler Ave., Tampa, Florida 33620

ABSTRACT

Reinforcing steel bars (~12mm diameter and 150mm long) were used in cyclic polarization tests in saturated $Ca(OH)_2$ solution and simulated concrete pore solution (SPS) with various levels of sodium chloride addition. Below a limiting chloride level (~0.004M $[Cl^-]$ in $Ca(OH)_2$ solution and ~0.4M $[Cl^-]$ in SPS solution), steel was not found to undergo pitting corrosion even if it was polarized to the oxygen evolution potential (~0.6V/SCE). At higher NaCl addition, pitting corrosion could often be initiated but the pitting potential was non-deterministic to a great extent. In $Ca(OH)_2$ solution, the average pitting potential was found to be strongly dependent on chloride concentration when $[Cl^-] \geq 0.008M$. In SPS solution, the average pitting potential was almost independent of the chloride concentration when $[Cl^-] \geq 0.8M$. The repassivation potential was found to be a strong function of the severity of corrosion attack that has occurred on the steel surface before repassivation, rather than a function of the chloride content of the bulk solution. The pitting tendency in chloride-containing SPS and $Ca(OH)_2$ solutions was interpreted on a statistical basis. The threshold thus determined for rebar in $Ca(OH)_2$ solution was in good agreement with other values reported in the literature.

Keywords: pitting, repassivation, rebar, cyclic polarization, $Ca(OH)_2$, SPS, threshold, chloride, hydroxide, potential, corrosion

INTRODUCTION

Reinforcing steel bars (rebar) in concrete are often corroded due to the chloride-induced breakdown of the protective passive film, when the chloride content of the concrete is high enough. It is generally believed that the free chloride in the concrete pore solution is responsible for the corrosion

Copyright
©1999 by NACE International. Requests for permission to publish this manuscript in any form, in part or in whole must be made in writing to NACE International, Conferences Division, P.O. Box 218340, Houston, Texas 77218-8340. The material presented and the views expressed in this paper are solely those of the author(s) and are not necessarily endorsed by the Association. Printed in the U.S.A.

initiation. Hydroxide ions in the pore solution play an opposing role and tend to stabilize the passive film. However, it is difficult to accurately determine the free hydroxide (OH^-) and free chloride (Cl^-) concentration in the concrete pore solution, especially at the rebar level. To gain insight on the relative proportions leading to corrosion initiation, several laboratory investigations[1-4] of the effect of OH^- and Cl^- on the corrosion behavior of reinforcing steel have been carried out in model alkaline solutions such as saturated $Ca(OH)_2$, pure NaOH or KOH solution, and simulated concrete pore solutions (SPS). Although it would seem easier to define the chloride corrosion threshold in a solution with controlled [OH^-] and [Cl^-] content, reported threshold values from different investigators have been in poor agreement. For example, steel remained passive in a pH 13.2 NaOH solution with 0.25M NaCl according to Hausmann[1], whereas Gouda[2] stated that the maximum tolerable chloride concentration was only 0.085M and 0.115M for NaOH solution with pH as high as 13.3 and 13.9, respectively. Discrepancies of this order merit additional study. This investigation used the cyclic polarization technique to determine the pitting and repassivation potentials of reinforcing steel in saturated $Ca(OH)_2$ solution and SPS solutions with various levels of NaCl. A statistical interpretation of the pitting potential was used to evaluate the chloride corrosion threshold concept and to establish a comparison with previous findings in the literature.

EXPERIMENTAL

Specimens ~150mm long were cut from ordinary A-615 reinforcing steel bars (size #4, diameter ~12mm) with diamond-pattern surface deformations. The chemical composition of the rebar steel used throughout this investigation is shown in Table 1. One end of the specimen was first drilled and tapped, then machined to produce a truncated conical shape. The conical bevel surface was then polished to 600 grit emery paper. The conical surface and the flat truncated end were then covered with a piece of plastic tubing before the rest of the specimen surface was sandblasted to remove the mill scale, after which the plastic tubing was removed and the specimen was stored in a dessicator. For testing, the specimen was assembled as shown schematically in Figure 1(a). The purpose of using such a design was to prevent crevice corrosion from happening, since preliminary tests with one end of the specimen mounted inside epoxy always produced crevice corrosion in the region bordering epoxy. The acrylic washer was very tightly pressed against the tip of the specimen by fastening the screw on the top of the assembly. The specimen had a nominal surface area of ~60 cm^2. Some of the specimens were used again, after freshly sandblasting the surface to remove all traces of corrosion from the previous experiment.

TABLE 1. CHEMICAL COMPOSITION OF THE REBAR STEEL

C	P	S	Mn	Si	Cr	Ni	Mo	Cu	Fe
0.43	0.007	0.038	1.11	0.22	0.03	0.11	<0.01	0.37	Bal.

The cell used in the experiments is schematically shown in Fig. 1(b). A rectangular tank (100mm×220mm×220mm) was sealed by clamping an acrylic glass lid onto its top opening, with a rubber gasket in-between. Four graphite rods (6mm×310mm) (two rods on each side of the tank) were symmetrically positioned with respect to the specimen, which was located in the middle of the tank. A saturated calomel electrode (SCE) was placed with the sensing tip ~10 mm away the specimen. All the measured potentials hereafter will be given with reference to SCE. The solution inside the tank was continuously deaerated by introducing commercially pure nitrogen at one end of the tank through a gas purger. The saturated calcium hydroxide solution was made with 2g/L reagent grade $Ca(OH)_2$ and distilled water. The simulated concrete pore solution (hereafter referred to as SPS, with a pH of ~13.6) was prepared according to Table 2. Pure sodium chloride was added into the solutions to adjust the chloride content. The total volume of the solution was ~4.6L for most of the tests.

TABLE 2. COMPOSITION OF THE SIMULATED CONCRETE PORE SOLUTION (SPS)

NaOH	KOH ☆	$Ca(OH)_2$*	pH
8.33 g/L	23.3 g/L	2 g/L	13.6

☆Reagent grade KOH had only a purity of 85.3%.

* Most of the $Ca(OH)_2$ was not dissolved.

Cyclic polarization tests were performed on the specimens with a forward (in the noble direction) scan rate of 0.167mV/sec. The polarization direction was reversed with a faster backward scan rate of 0.417mV/sec once the nominal anodic current density had reached 100μA/cm^2. The faster backward scan rate was used to lessen the severity of corrosion created on the steel surface[4]. A much slower forward scan rate (0.0167 mV/sec) was also used in selected tests to establish how dependent were the results on the choice of forward scan rate. Before applying the cyclic polarization schedule, each specimen was conditioned at −1V for 2000 seconds to remove any oxide films that may have existed on the specimen surface. The cyclic polarization tests were repeated 14 to 18 times in SPS solution and 3 to 5 times in $Ca(OH)_2$ solution at each specific chloride addition. A newly surfaced specimen was used each time.

RESULTS

Cyclic polarization in SPS solution

Fig 2. shows several typical cyclic polarization curves for steel specimens in SPS solution with 0.6M NaCl addition. The passive plateau current density before pitting initiation was ~6μA/cm2 and generally reproducible (assuming interfacial capacitance ~100μF/cm^2 [5] the charging current due to the interfacial capacitance during the potentiodynamic scan was estimated to be on the order of 0.02 μA/cm^2 and hence negligible). This passive plateau current density is much higher than the normal steady state passive current density of steel in such a environment since the anodic polarization was performed dynamically and finished within only ~3 hours. As a result, a steady state passive film was unlikely to be produced. The surge in current density at ~0.6V was likely due to the oxygen evolution process, as expected from the H_2O electrochemical stability diagram[6].

The various types of behavior of steel specimens exemplified in Fig. 2 can be categorized into three modes. In the first mode (run #2) pitting was not initiated up to the oxygen evolution potential. In the second mode (run #4) pitting was initiated at a high potential (but below the oxygen evolution potential); pitting was initiated normally during the forward scan but in some instances initiation took place during the reverse scan. In the third mode (run #1 and #3) pitting was easily initiated at potential as low as -0.1V. In the second and third modes where stable pitting was initiated, a large hysteresis loop could be observed. For chloride concentrations of 0.4M or lower, the specimens behaved as in the first mode. For chloride concentrations higher than 0.8M, the behavior was usually as in the third mode, although the pitting initiation potential varied significantly from test to test, as will be shown later. For intermediate concentrations (as is the case in Figure 2, for 0.6M NaCl), all three modes could be observed, varying unpredictably from test to test.

Fig 3. shows examples of cyclic polarization curves for steel specimens in SPS solution with 1.5M NaCl addition at a forward scan rate of 0.0167mv/sec. The passive plateau current densities before pitting initiation shown in Fig. 3 were ~8 times lower than those shown in Figure 2 for tests conducted at 0.167 mV/sec. This result strongly suggests that a more stable or thicker passive film was formed at the slower scan rate. However, the pitting behavior shown in Fig. 3 differed little from that obtained with 10

times higher scan rate in the same solution. The average pitting potentials at these two different scan rates differed only by ~40mV. This suggests that the scan rate of 0.167mv/sec used in the rest of the experiments was reasonably away from a domain of large scan rate dependence of the pitting potential.

Cyclic polarization in saturated $Ca(OH)_2$ solution

Fig. 4 shows several typical cyclic polarization curves for steel specimens in saturated $Ca(OH)_2$ solution with different levels of chloride addition. The behavior of steel at various level of NaCl addition followed comparable trends (but at different concentration regimes) to those observed in the SPS tests. Below 0.004M chloride addition, no pitting was initiated up to the oxygen evolution potential (~0.6V). At chloride addition higher than 0.008M, pitting was generally initiated more easily at more active potentials, although the pitting initiation potential again varied from test to test even in the same solution.

Effect of chloride content on pitting and repassivation potentials

Fig. 5 shows the relationship between the pitting and repassivation potentials and the chloride concentration in SPS and $Ca(OH)_2$ solutions. The pitting potential (hereafter called Ep) for each measurement was defined as the potential at which the nominal anodic current density reached $10\mu A/cm^2$. If pitting corrosion was not initiated in a test (such as those performed in SPS solution with less than 0.4M NaCl or in $Ca(OH)_2$ solution with less than 0.004M NaCl), the potential corresponding to an current density of $10\mu A/cm^2$ in the oxygen evolution range was reported as if it were the actual Ep. The arrows in Fig. 5 indicate that the actual Ep in those cases was likely higher than that the reported value. The relationship between the chloride concentration in the SPS solution and the repassivation potentials (hereafter called Er) from the same series of cyclic polarization tests are also shown in Fig. 5. Er was defined as the potential on the cyclic polarization curve where the backward scan intersected the forward scan. The averages of Ep (solid lines) and averages of Er (dashed lines) are shown for comparison.

In SPS solution, both Ep and Er experienced a sharp transition from 0.4M NaCl to 0.8M NaCl. During that transition, both Ep and Er were widely scattered, compared with these observations at lower or higher chloride concentrations. When the chloride concentration was higher than 0.8M, Ep was almost chloride concentration independent, although Ep varied from –0.3V to +0.1V. Er behaved in a similar way at those chloride concentrations. In SPS with 0.6M chloride, Er in two cases was even higher than Ep obtained in other repeat tests of the same series. This behavior will be discussed later.

The variations of Ep and Er were less severe in the limited number of tests performed in $Ca(OH)_2$ solution. When chloride concentration was higher than 0.01M, Er was nearly chloride concentration independent. However, the average Ep was approximately in inverse linear relationship with the logarithm of chloride concentration.

DISCUSSION

In both SPS and $Ca(OH)_2$ solutions the pitting potential was far from a unique value at any given chloride concentration, and the results tended to cluster around different values at different chloride concentrations. In that sense, a clearly defined chloride concentration threshold or potential threshold does not seem to exist. However, the results appear to be compatible with the presence of a limiting chloride threshold, defined as the highest chloride concentration that can be tolerated without causing

pitting corrosion of the rebar steel up to the oxygen evolution potential. This limiting threshold would be ~0.4M [Cl-] in SPS and ~0.004M [Cl-] in $Ca(OH)_2$ solution, respectively. At higher chloride concentrations, the behavior of steel could only be predicted on a statistical basis. To that effect Figs. 6 and 7 show the pitting and repassivation probability of rebar steel in SPS and $Ca(OH)_2$ solutions, respectively, at various chloride levels. The pitting or repassivation probability was defined as the ratio of the number of specimens (~60 cm^2 each) that had been pitted or repassivated under the specified potential, to the total number of specimens that had been tested in a given solution.

In SPS solutions below –0.3V, the pitting probability was very small in the investigated chloride concentration range. However, for chloride concentrations ≥ 0.8M, the pitting probability was ~50% when the potential was ~-0.1V. Since the open circuit potential of rebar steel in SPS solution before pitting initiation is normally near that value, steel under those conditions seems to have a very high pitting chance if enough time is given to allow the nucleation of a stable pit. It is uncertain whether at 0.6M NaCl addition steel could be pitted naturally, as the lowest Ep (among 14 repeat tests) was very close to the open circuit potential of steel in that solution. Since it is reasonable to expect the lowest Ep to shift toward more negative values if a larger number of repeat tests were to be conducted (comparable to considering a larger steel surface area), the chances for pitting may be greater than they appear to be now. The extent to which the lowest Ep can shift toward more active potentials upon increasing the number of tests has not been determined at present.

The results in Fig. 7 for the pitting and repassivation probability of steel in $Ca(OH)_2$ solutions can be examined in a similar manner as those for the SPS solutions, keeping in mind that the data set is much smaller. By using the same criteria as indicated above, steel had a very high pitting probability at the open circuit potential when the chloride concentration exceeded 0.04M. The pitting probability increased with the chloride concentration. The pitting probability of steel in $Ca(OH)_2$ solution with 0.1M NaCl approached 100%. On the other hand, the pitting probability at much lower NaCl levels (less than 0.01M) was expected to be negligible at the corresponding open circuit potential of ~-0.1V. In that sense, the limiting chloride threshold in $Ca(OH)_2$ solution would be somewhat between 0.01M and 0.04M. Interestingly, by immersing a set of 12 mild steel rod specimens in chloride-containing $Ca(OH)_2$ solution at open circuit potential for ~2 weeks, Hausmann[1] found that the pitting probability of steel was ~0% at 0.02M NaCl and ~100% at 0.1M NaCl, respectively. The present findings are in very good agreement with Hausmann's results.

To our knowledge, most of the cyclic polarization or potentiodynamic polarization tests reported in the literature to determine the pitting potential have been performed on steel specimens with small surface area (typically ≤ 5cm^2). Due to the non-deterministic nature of the pitting potential, interpretation of experimental results based only on single or duplicate tests can be misleading, especially when a test is performed near transition conditions, such as SPS with 0.6M NaCl. Studying the pitting potential of 304 and 316 stainless steel in 3.5% NaCl (~0.6M) solution with a potential sweep (0.333mV/sec) method, Shibata and Takeyama[7] found that a large ensemble of pitting potential values followed a normal distribution and that the maximum pitting potential variations was 0.35V in a population of 20 specimens with ~0.2 cm^2 exposed surface area each. However, Wilde[8] found using larger specimens (5 cm^2) that the pitting potential of 304 SS in 1M NaCl solution could be reproduced to ±10mV on triplicate runs. Those results strongly suggest the presence of an area effect on the pitting initiation potential. It may be therefore expected that the pitting potential obtained from a larger specimen (or the lowest Ep from numerous repeated tests on small-sized specimens) may be more representative of the pitting potential prevalent in a large steel area as it may be found in actual structures. The above considerations inspired the use of larger specimens and multiple test in the present investigation and ongoing continuation studies.

Figs. 6 and 7 for probability show significant scatter in the repassivation potential Er. This is consistent with previous studies showing Er to be far from a unique value[9,10]. The maximum variation of Er (~1.3V) was found for steel in SPS with 0.6M NaCl. The sensitivity of Er to test conditions is evident when Er is plotted against the maximum corrosion current (i_{max}) recorded during the cyclic polarization test (Fig.8). All the data in Fig. 8 come from the numerous cyclic polarization tests performed in $Ca(OH)_2$ and SPS solution with various levels of chloride addition (the figure includes only those tests in which the corrosion current could be clearly separated from the oxygen evolution current). It can be seen that Er is a strong function of the severity of corrosion attack (expected to be an indicator of the depth of the pit created during the test) that has occurred on the steel before repassivation, rather than a function of the chloride content of the bulk solution. This result is in good agreement with the findings by Dunn et al[9], who reported a similar relationship between Er and maximum pitting penetration depth. The observation in that work that Er of a shallow pit can be several hundred milivolts higher than Er of a deep (more stable) pit may reasonably explain why in certain cases the Er values obtained in SPS solutions with 0.6M NaCl were even higher than the Ep values from other repeat tests in the same series. Generally, for $i_{max}>100\mu A/cm^2$, Er was approximately in inverse linear relationship with log i_{max}. Similar behavior has also been reported by Wilde[10] for type 430 stainless steel in 1M NaCl solution. This strong dependence of Er in experimental conditions obscures the applicability of the repassivation potential measurement as a means to evaluate critical conditions for corrosion initiation of reinforcing steel in alkaline media.

CONCLUSIONS

- Below a limiting chloride level (~0.004M [Cl^-] in $Ca(OH)_2$ and ~0.4M [Cl^-] in SPS solution), steel was not found to undergo pitting corrosion up to the oxygen evolution potential (~0.6V/SCE).
- The pitting potential was found to be non-deterministic; the extent of its variation was strongly chloride concentration dependent.
- The repassivation potential was found to be mainly related to the severity of the corrosion that had been initiated during the cyclic polarization process.
- A simple statistical analysis was used to evaluate the pitting and repassivation tendency of rebar steel in $Ca(OH)_2$ and SPS solution.
- The threshold determined from the pitting probability distribution curve for steel in $Ca(OH)_2$ solution was in agreement with other values reported in the literature.

ACKNOWLEDGMENT

This work was supported by the Florida Department of Transportation. The opinions, findings and conclusions expressed here are those of the authors and not necessarily those of the supporting agencies.

REFERENCES

1. D.A. Hausmann, Mater. Protection, 6, 11(1967): p.19
2. V.K. Gouda, Br. Corrosion. J., 5, 9(1970): p.198
3. W. Breit, Materials and Corrosion,49, (1998): p539
4. N. S. Berke, "The Use of Anodic Polarization to Determine the Effectiveness of Calcium Nitrite as an Anodic Inhibitor," Corrosion Effect of Stray Currents and the Techniques for Evaluating Corrosion of Rebars in Concrete, ASTM STP 906, V. Chaker, Ed., American Society for Testing and Materials, Philadelphia, 1986, pp.78-91,

5. A. A. Sagüés, "Electrochemical Impedance of Corrosion Macrocells on Reinforcing Steel in Concrete," CORROSION/90, paper No.132,(Houston,TX: NACE International,1990)
6. M. Pourbaix, Lectures on Electrochemical Corrosion, third English Edition, NACE International, Houston,1995, p19
7. T. Shibata, and T. Takeyama, Corrosion, 33,7(1977):p.243
8. B.E. Wilde and E. Williams, J. Electrochemical Soc., 116,11(1969): p.1539
9. D.S. Dunn, N. Sridhar, and G.A. Cragnolino, Corrosion, 52,2(1996): p.115
10. B.E. Wilde, Corrosion, 28, 8(1972): p.283

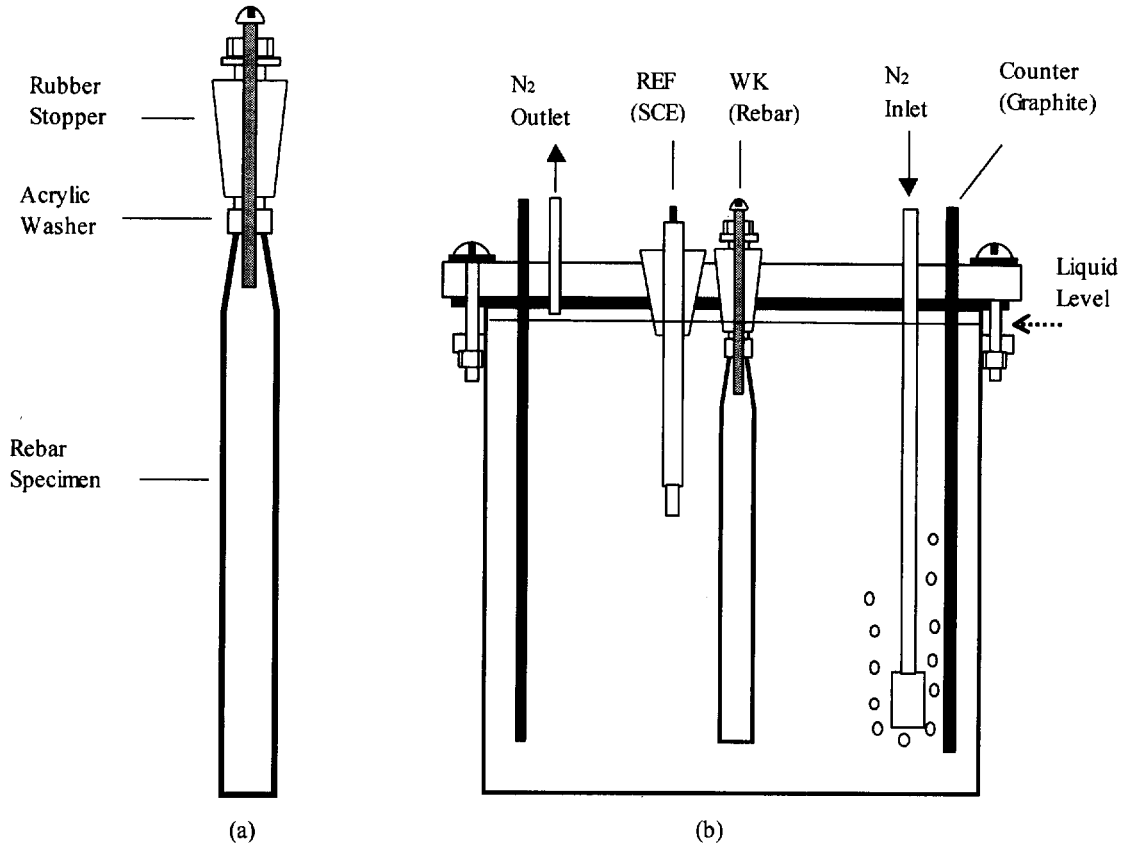

FIGURE 1 - Schematic graph showing the assembly of the specimen (a) and the cell (b) used in the experiments

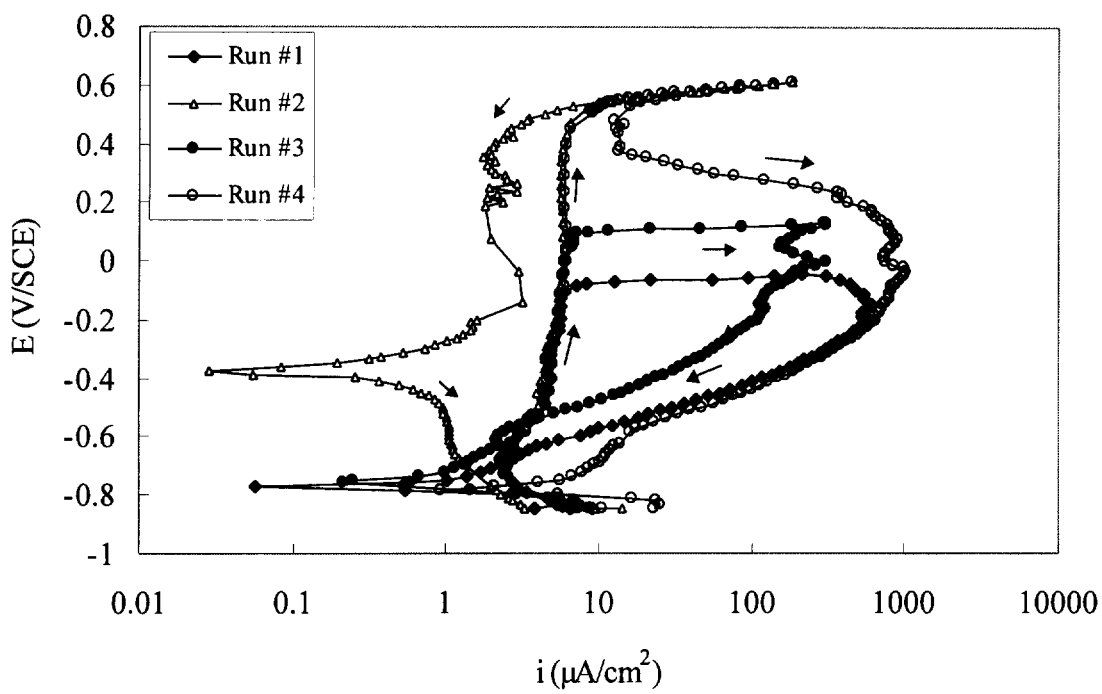

FIGURE 2 - Cyclic polarization curves of rebar steel in SPS solution with 0.6M NaCl

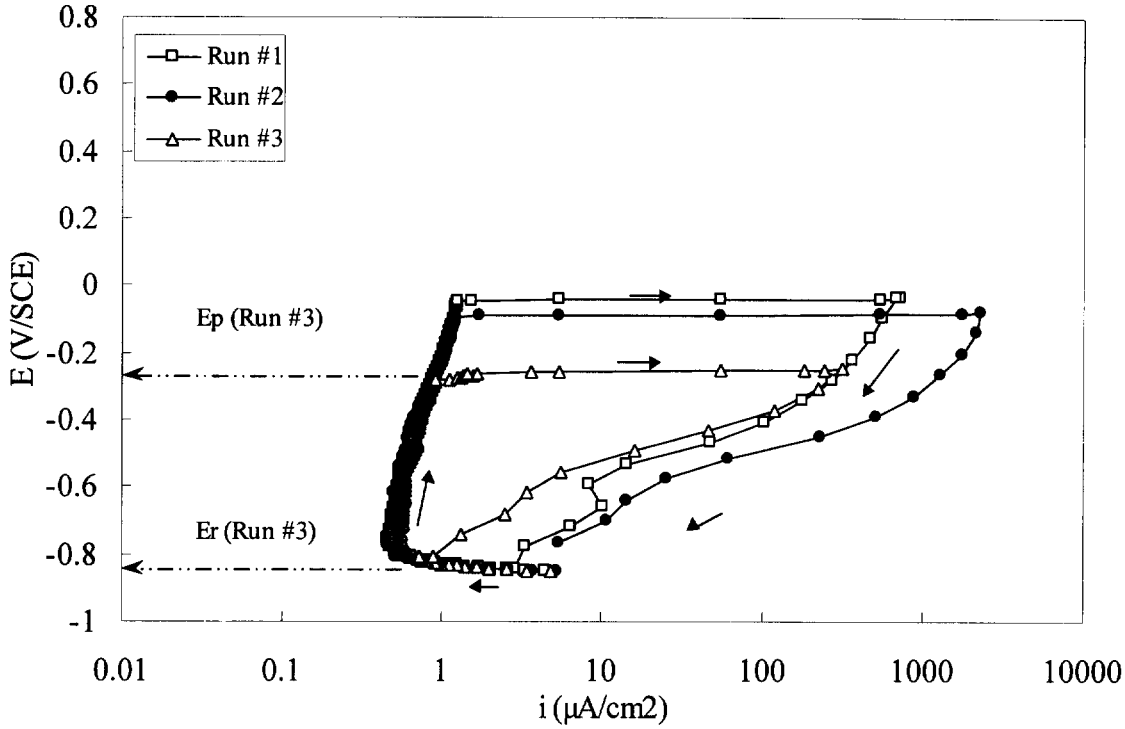

FIGURE 3 - Cyclic polarization of rebar steel in SPS solution with 1.5M NaCl (scan rate: forward 0.0167mV/sec, backward 0.417mV/sec). (Ep and Er for Run #3 are exemplified as shown.)

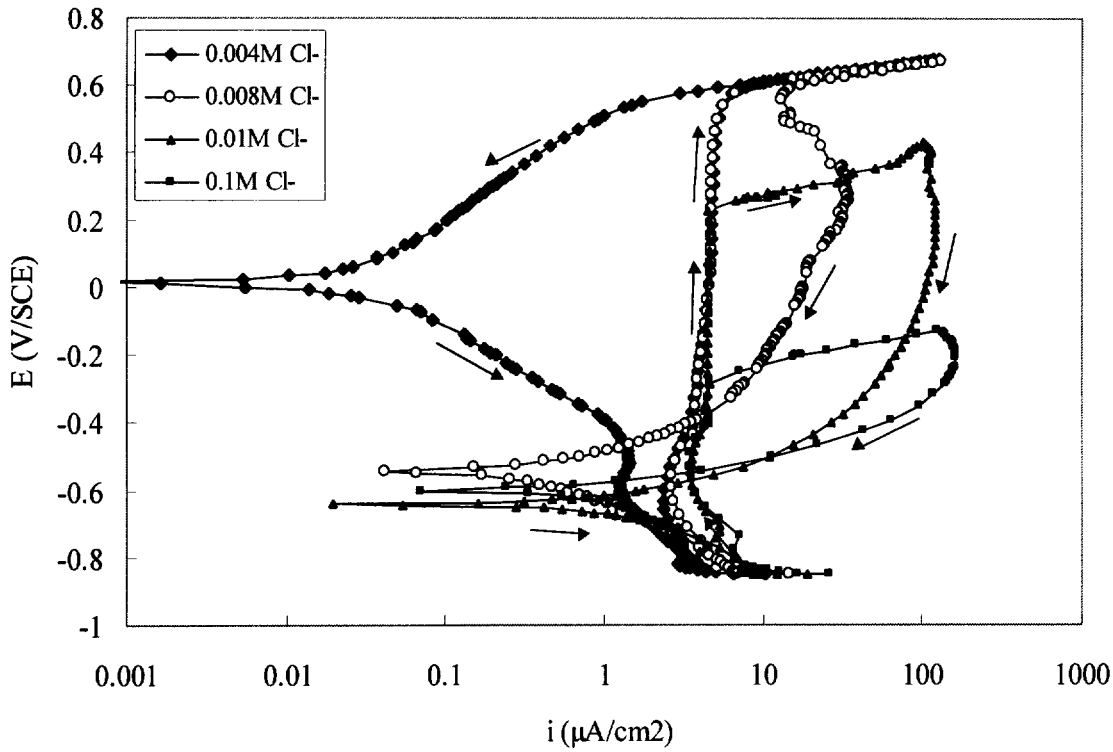

FIGURE 4 - Typical cyclic polarization curves of rebar steel in $Ca(OH)_2$ solution with various levels of NaCl

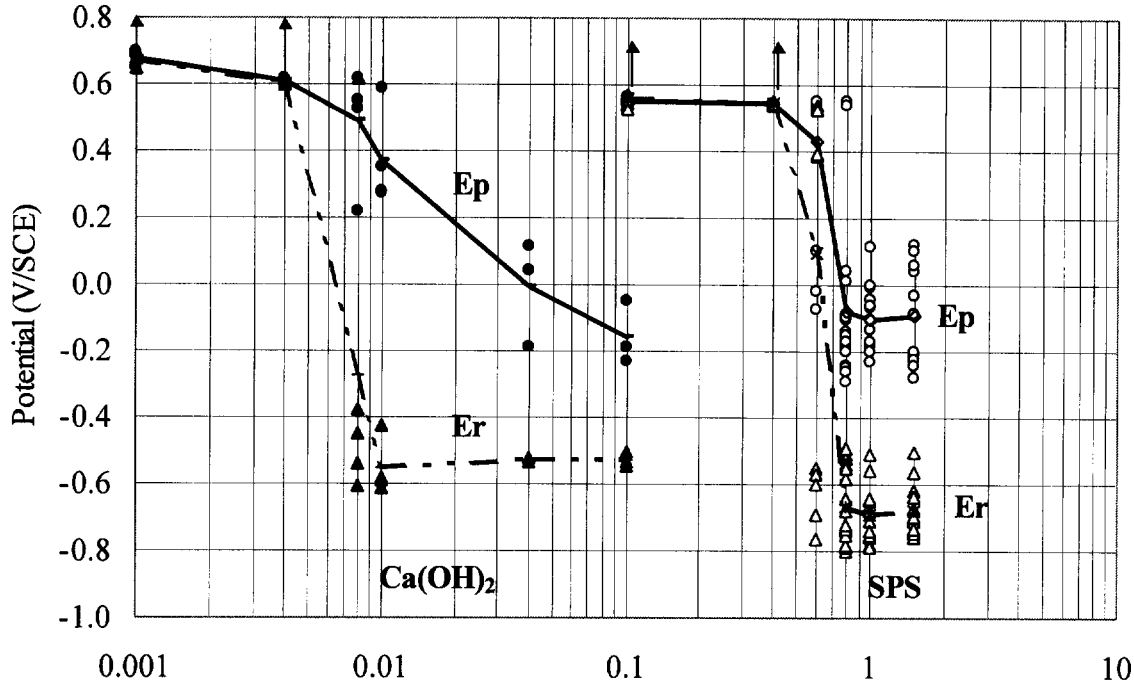

FIGURE 5 - Relationship between Ep, Er and chloride concentration in $Ca(OH)_2$ and SPS solutions

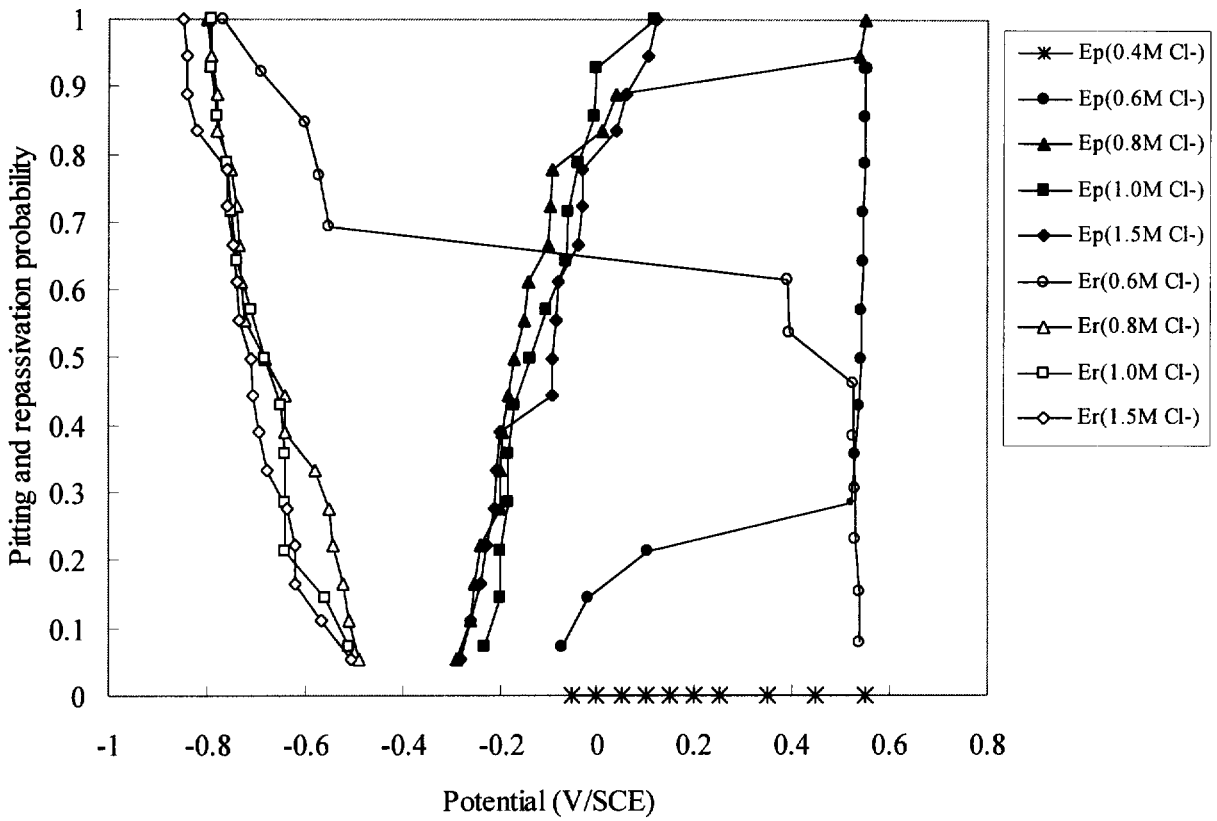

FIGURE 6 - Pitting and repassivation probability of rebar steel in SPS with various levels of NaCl

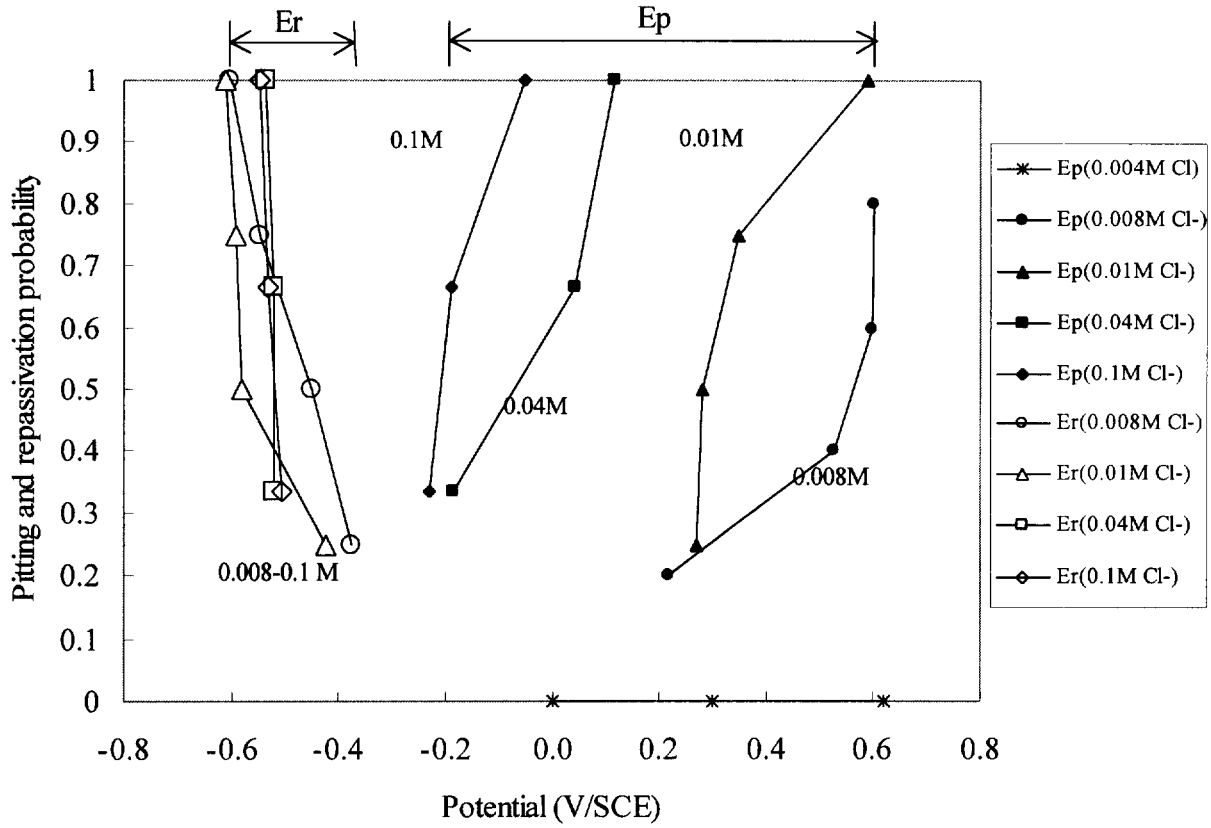

FIGURE 7 - Distribution of pitting and repassivation probability versus potential in $Ca(OH)_2$ solution with various levels of NaCl

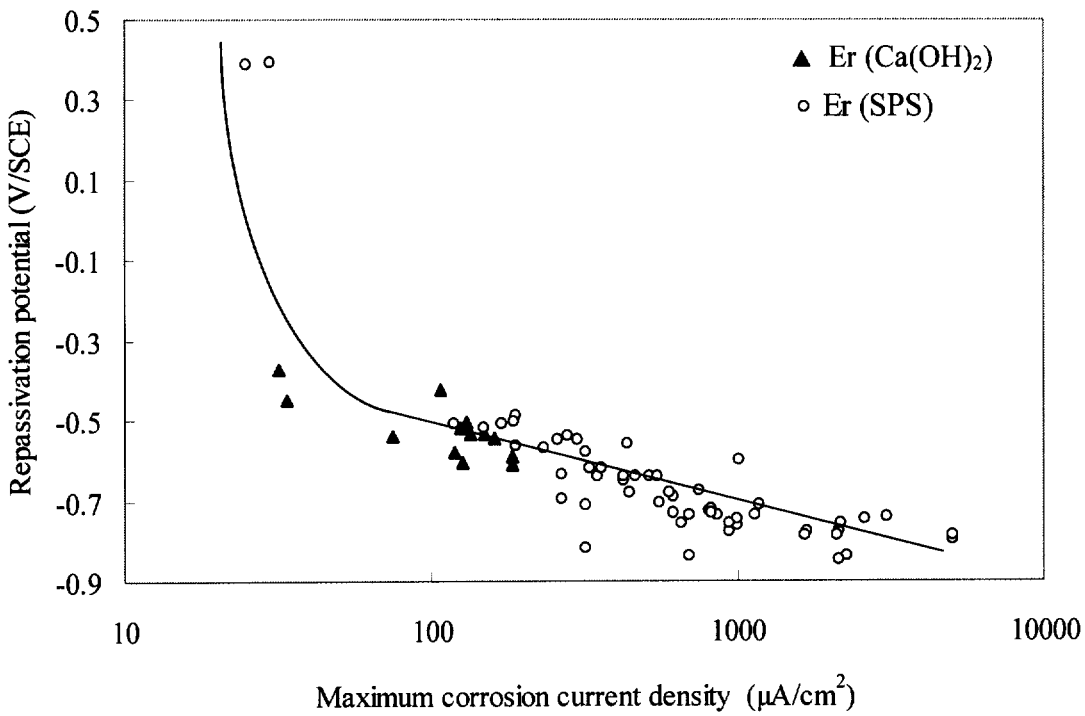

Figure 8 - Relationship between repassivation potential (Er) and maximum corrosion current density (i_{max})